Journal of Materials Science and Engineering with Advanced Technology
Volume 1, Number 1, 2010, Pages 81-96

STUDY ON A NEW METHOD FOR THE PREPARATION OF NANO-CERIA POWDER OF HIGH THERMAL STABILITY

FENG-YUN WANG[1], GUO-BIN JUNG[2], SHI-JUN LUO[3], CHANG-LING WANG[1], XIAO HAO[1], CHI-YUAN LEE[2] and FENG-BOR WENG[2]

[1]School of Chemistry
Huazhong Normal University
Wuhan, Hubei 430079
P. R. China
e-mail: sxwfy@hotmail.com

[2]Fuel Cell Center and Department of Mechanical Engineering
Yuan Ze University
Chungli, Taoyuan County 320
Taiwan

[3]School of Science
Hubei University of Automotive Technology
Shiyan, Hubei 442002
P. R. China

Abstract

A new method for the preparation of nano-ceria of high thermal stability was systematically studied by using XRD, TEM, ICP-AES, N_2 physical adsorption and desorption, and an equipment combining the functions of thermal gravimetry, differential scanning calorimeter, and mass spectrometer. The method includes the synthesis of MgO-CeO_2 mixed powder by calcining a gel made with cerium nitrate, magnesium nitrate, and citric acid, and the removing of MgO from the

Keywords and phrases: ceria preparation, MgO, thermal stability, new method.

Received November 27, 2009

mixed powder by acetic acid leaching. The calcining process mainly included two weight-loss steps. Step 1 took place at a lower temperature, which decreasing from 535K to 480K slightly with Mg/Ce increasing from 1 to 14, probably due to the reaction between the organic fragments and nitrogen oxides from the nitrates, and the catalytic function of MgO. Step 2 took place at a higher temperature, which increasing from 620K to 740K apparently with Mg/Ce increasing, due to the reaction between the organic fragments and O_2, and the catalytic function of CeO_2. The MgO in the mixed powder could be completely removed by reaction with acetic acid solution (2.5 vol.%) at room temperature, but the CeO_2 remained unaffected. In the calcining process, the freshly formed ceria particles could thermally be stabilized in the rest calcining, but did not agglomerate because the formed MgO particles might act as isolators. Consequently, the resulting ceria powders showed high surface area and high thermal stability.

1. Introduction

As a functional rare earth material, ceria has wide applications in electrochemistry, optics, and catalysis due to its unique properties [8-10, 12]. For instance, ceria doped with other rare earth ions has high oxide ion conductivity at a comparable low temperature (about 873K), and thus has been applied in solid oxide fuel cells [8]. Ceria has strong absorption in the ultraviolet range and is used as ultraviolet (UV) blocking materials [9, 10]. Ceria has been used in the three-way catalyst (TWC) for exhaust gas treatment from automobiles because of its high oxygen storage capacity, associated with its rich oxygen vacancies, and low redox potential between Ce^{3+} and Ce^{4+}[11, 12]. Ceria has also been widely used as catalysts or catalyst supports for reactions of oxidation [6], steaming reforming [15], and water-gas shift [5].

Ceria can be prepared by various methods, such as hydrothermal [13] or microwave-hydrothermal synthesis [3], solvothermal [2] or microwave-assisted solvothermal synthesis [18], homogeneous precipitation [14], decomposition [7], sonochemical treatment [17], and so on. Usually, different methods resulted in different ceria for different applications. Although, surface area is important for almost all applications, thermal stability is more important for such applications at high temperature. For instance, the ceria in the three-way catalyst needs to be thermally stable

at about 1173-1273K [11]. Nevertheless, the ceria prepared with the available methods are not thermally stable enough at such high temperature. In a US patent [20], a ceria was prepared by precipitating cerium nitrate with ammonium hydroxide. While the ceria had a surface area of 218m^2/g after calcination at 700K for 4 hours in air, the surface area dropped to 4m^2/g following 4 hours calcination at 1255K. In another US Patent [21], a ceria was prepared by refluxing ammonium ceric nitrate with ammonium sulphate for 24 hours to obtain a hydrous ceria powder. Following calcination at 811K in air for 4 hours, this ceria maintained a surface area of 150m^2/g. However, only 5m^2/g of surface area left, if the calcining temperature was raised to 1253K [22].

In our previous paper [16], a new method was briefly reported for the preparation of nano-ceria powder of high thermal stability. The obtained ceria remained a surface area as high as 25.1m^2/g, even after being annealed at 1253K for 4 hours. In this work, the details of this new method were systematically studied, and its mechanism was discussed.

2. Experimental

2.1. Ceria preparation

Preparation of ceria with the new method includes two steps: (1) preparing CeO_2-MgO mixed powder by sol-gel method, and (2) removing MgO by selective acid leaching.

The starting materials were the nitrate salts of reagent grade (Acros) and used as purchased. The aqueous solutions of each metal ion of Ce^{4+} and Mg^{2+} were prepared by dissolving the nitrate salt in distilled water, and diluting them to desired concentrations. An aqueous solution of citric acid (CA) and polyethylene glycol (PEG) in a weight ratio of $\mathrm{CA/PEG} = 60$ was also prepared and termed as CP solution. According to the designed molar ratios of Mg/Ce (termed as x, where $x = 0\text{-}14$), different volumes of metal ion solutions were taken and mixed in a beaker. Then, CP solution was added in the beaker, until the molar

number of citric acid was equal to the total number of the metal ions in the beaker. The mixed solution was evaporated under stirring at 353K, until the solution became viscous gel which was then dried at 378K, ground, and termed as N(*x*)-CeMgCP. The dried gel was calcined in air at a given temperature (*Tc*, 723-1253K) for 4 hours, and then ground again to form CeO_2-MgO mixed powder [termed as N(*x*)*Tc*-CeMg].

To remove MgO, a calcined sample N(*x*)*Tc*-CeMg was added into a beaker, which had contained 2.5 vol. % acetic acid solution, until the ratio of the solution/powder reached 200ml/g. The slurry was stirred at room temperature for 30min, then filtered and washed with distilled water, and then dried at 378K over night. The obtained CeO_2 sample was termed as N(*x*)*Tc*-CeO_2. This sample was, then annealed in air at a temperature of *Ta* (393-1253K) for 4 hours, and termed as N(*x*)*Tc*/*Ta*-CeO_2 .

2.2. Sample characterization

The calcining process of dried gel N(*x*)-CeMgCP was in-situ investigated on an equipment (TG-DSC-MS, NETZSCH STA 409C/CD) combining thermal gravimetry (TG) , differential scanning calorimeter (DSC), and mass spectrometer (MS) with air flow rate of 30cm^3/min, temperature range of 293-1073K, and temperature ramp of 10K/min. The composition of the mother-solution from the acid leaching process, and all solid samples were analyzed on an inductively coupled plasma-atomic emission spectrometer (ICP-AES, Jarrell-Ash ICAP9000). The crystal phases of CeO_2-MgO mixed powders, and all CeO_2 samples were identified at room temperature by using a *X*-ray diffractometer (XRD, Rigaku/MAX-II, Cu Kα radiation), and the crystallite size of the ceria samples were measured with XRD line-broadening method. The surface area (S_g) of the ceria samples were determined with a micromeritics ASAP 2000 apparatus using nitrogen as the analysis gas. Transmission electron microscopy (TEM, Hitachi H-7100, 100keV) were used to measure the particle size of the ceria samples.

3. Results and Discussion

3.1. Gel formation and calcination

3.1.1. Gel formation

The gel was formed by evaporating the mixed aqueous solution of cerium nitrate, magnesium nitrate, and citric acid (H4L). In this solution, complexes containing L, Ce^{3+}, and/or Mg^{2+} should be formed. When evaporating the solution, water steam and brown gas (possibly NO_2 from nitric acid or nitrate) were gradually released; polymerization among the different complexes as well as citric acid might take place; and therefore, viscous gel was formed. When further drying, evaporation and polymerization continued, and dried gel was formed.

3.1.2. Gel calcination

The thermal behavior of the dried gels N(x)-CeMgCP with x = 1-14 were investigated by TG equipment, and the obtained TG curves were shown in Figure 1. Each curves showed two notable weight-loss steps, marked as step1 for the lower temperature (T_1) and step 2 for the higher temperature (T_2). As shown in Figure 2, the step temperature decreased with x for step1 according to the Equation (1), but increased for step 2 according to the Equation (2).

$$T_1 = 752 - 148.43\ \mathrm{EXP}(-x / 6.2626), \quad (1)$$

$$T_2 = 605 - 1.3545\,(1 - \exp(-x / 0.00702)) + 148.42675\,(1 - \exp(-x / 6.2695)). \quad (2)$$

The Equations 1 and 2 were obtained by curve fitting with $R^2 \geq 0.996$. From Figure 1, the lowest temperature ($T_{lc,}$) for complete combustion of each gel sample was measured, and was found increasing from 629K to 773K with x from 1 to 14.

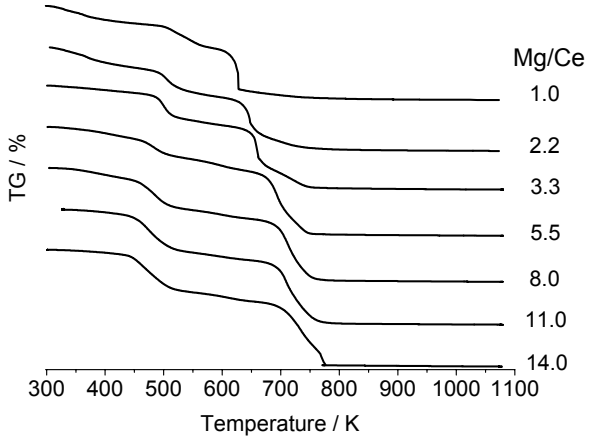

Figure 1. TG profiles of gel samples N(x)-CeMgCP with x = 1-14 (293-1073K, 10K/min, air 30ml/min).

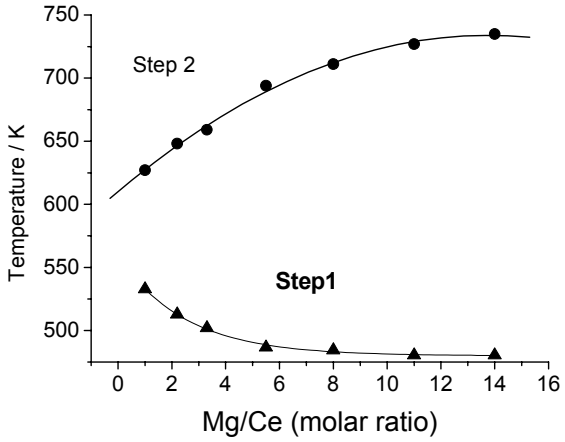

Figure 2. Effect of Mg/Ce(x) on the weight-loss temperatures of TG profiles for the gel samples N(x)-CeMgCP with x = 1-14.

For deeply understanding the weight-loss steps, the calcination process of the dried gel N(5.5)-CeMgCP was in-situ investigated with TG-DSC-MS equipment. Figure 3 shows the TG and DSC curves, and Figure 4 shows the MS profiles. Two weight-loss steps were observed. Step1 took place at 489.5K, with a little broad exothermic peak in DSC curves, and a little broad peak at the mass of 44 in the MS profiles. Step 2 took place at 693K, with a sharp exothermic peak in DSC curves, and a sharp peak at the mass of 44 in the MS profiles. The marked difference between steps 1 and 2 indicate that the mechanisms for steps 1 and 2 must be different, and the released-matters from steps 1 and 2 might also be different even though, they had the same mass of 44. The lost-matter from step 2 should be CO_2, which was produced from the reaction between the organic fragments remained in the sample and oxygen in air. This oxidation reaction is usually strongly exothermic, and can be catalyzed by CeO_2 [1], therefore, the reaction temperature increased with x increasing. The released-matter from step 1 might be N_2O, which was produced possibly from the reaction between organic fragments remained in the sample and nitrogen oxides (NOx, x = 1-2.5) derived from the nitrates. This reaction might be weakly exothermic, and might be catalyzed not by CeO_2, but by MgO in some extent. Therefore, the reaction temperature slowly decreased with x increasing. Further studies are required to clarify the mechanism for step 1.

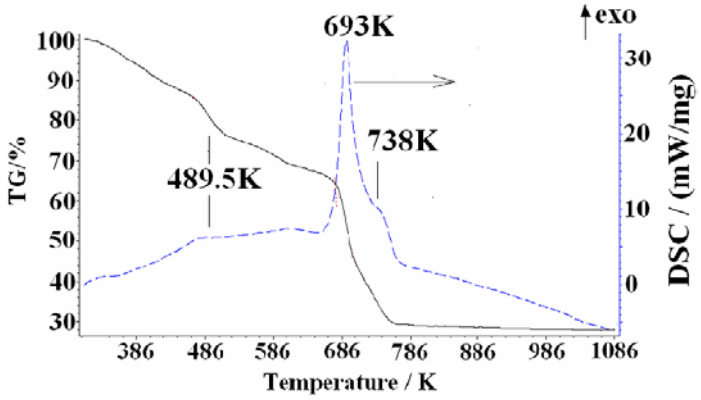

Figure 3. TG-DSC profiles of the gel sample N(5.5)-CeMgCP (293-1073K, 10K/min, air 30ml/min).

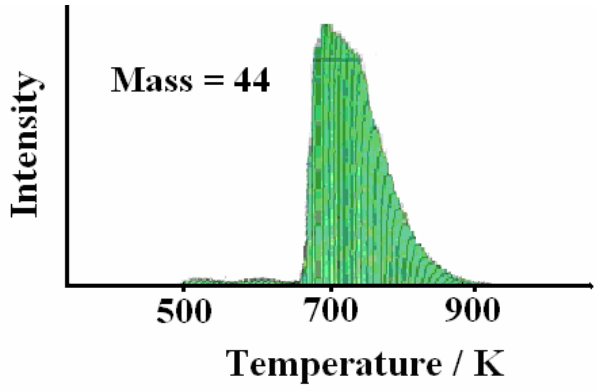

Figure 4. Mass spectrum of gel sample N(5.5)-CeMgCP as a function of calcining temperature (293-1073K, 10K/min, air 30ml/min).

Figures 5a and 5b show the XRD patterns of the calcined samples N(x)773-CeMg with x = 1.0-5.5, and N(x)1253-CeMg with x = 5.5-14. The two figures are quite similar. Only MgO and CeO_2 phases were observed for all the Mg containing samples except for x = 1.0. The CeO_2 phase in the Mg containing samples has the same XRD peak positions as the pure CeO_2 sample, indicating that no detectable Mg^{2+} entered the CeO_2 lattice. This is understandable because even at 1873K, the solubility of MgO in the CeO_2 lattice was only 2% [4]. Since the XRD signal of MgO is relatively weak, the XRD peaks of MgO in the lowest Mg-containing sample of x = 1.0 might be too weak to be detected out. The above XRD results indicate that after calcinations, the dried gels became the mixed powder of CeO_2 and MgO.

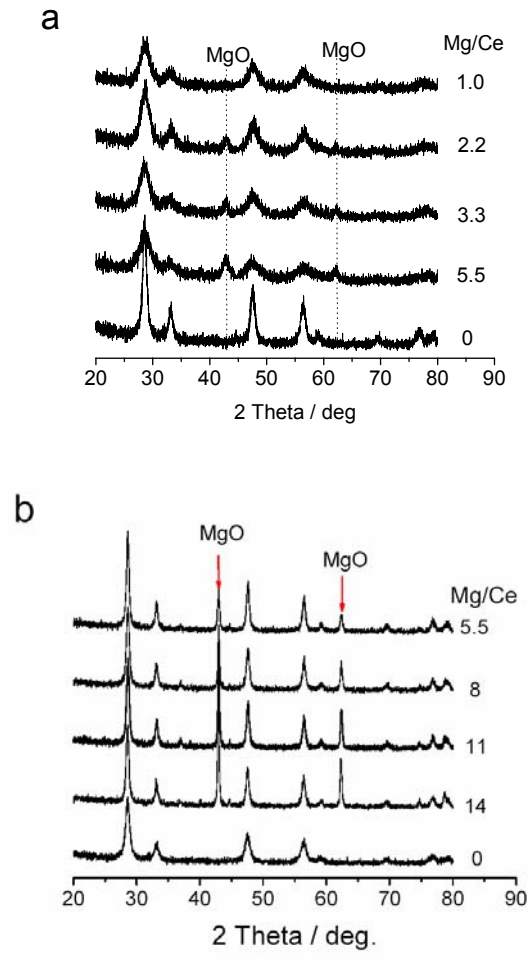

Figure 5. XRD patterns of calcined samples of (a) N(x)773-CeMg with x = 1.0-5.5, and (b) N(x)1253-CeMg with x = 5.5-14, Cu Kα radiation.

3.2. MgO removing

MgO in the MgO-CeO_2 mixed powders was removed by selective acid leaching, where MgO reacted with acetic acid solution and formed solvable magnesium acetate, but CeO_2 remained unchanged. Figure 6 shows the XRD patterns of the leached samples of (a) N(x)773/773-CeO_2 with x = 1.0-5.5, and (b) N(x)1253/378-CeO_2 with x = 5.5-14. For all the samples, only CeO_2 phase was observed, indicating that MgO phase was

removed. Considering XRD signal is not very sensitive for MgO, the composition of a representative leached sample N(1.0)973/973-CeO_2 was analyzed with ICP-AES. Ce was observed, but no Mg was detected out, suggesting that MgO was completely removed. The composition of the mother-solution from the acid leaching process was also analyzed with ICP-AES. The ratio of Mg/Ce was found more than 800, indicating that the effect of acid leaching on CeO_2 phase is negligible.

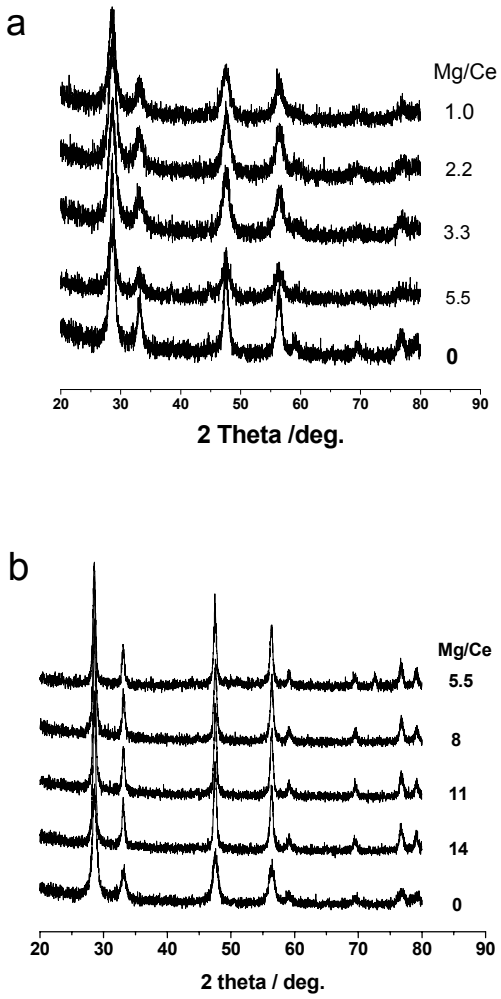

Figure 6. XRD patterns of leached samples (a) N(x)773/773-CeO_2 with x = 1.0-5.5, and (b) N(x)1253/378-CeO_2 with x = 5.5-14, Cu Kα radiation.

Using XRD line-broadening method, the crystallite size of the ceria samples of N(x)Tc/Ta-CeO_2 were measured, and was found decreasing with x increasing and approaching constant when $x \geq a$ given value of x_0. Besides, the x_0 increased with Tc and Ta. For instance, when $Tc = Ta = 773\text{K}, x_0$ was about 2.2, and the ceria crystallite sizes for x = 2.2-5.5 were between 5.9-6.2nm. When $Tc = Ta = 1253\text{K}$, the x_0 was about 5.5, and the ceria crystallite sizes for x = 5.5-11 were between 24-28nm.

The particle sizes of the ceria samples N(x)773/378-CeO_2 with x = 1.0-5.5 was measured from the TEM micrographs (Figure 7), and shown in Figure 8 as a function of x. For all the samples, the particles were in sphere-like shape and the average particle size decreased with x increasing, and approached constant when $x \geq 3.3$, indicating that the existing of MgO hampers the CeO_2 crystallite from agglomerating, but too much MgO seems not necessary.

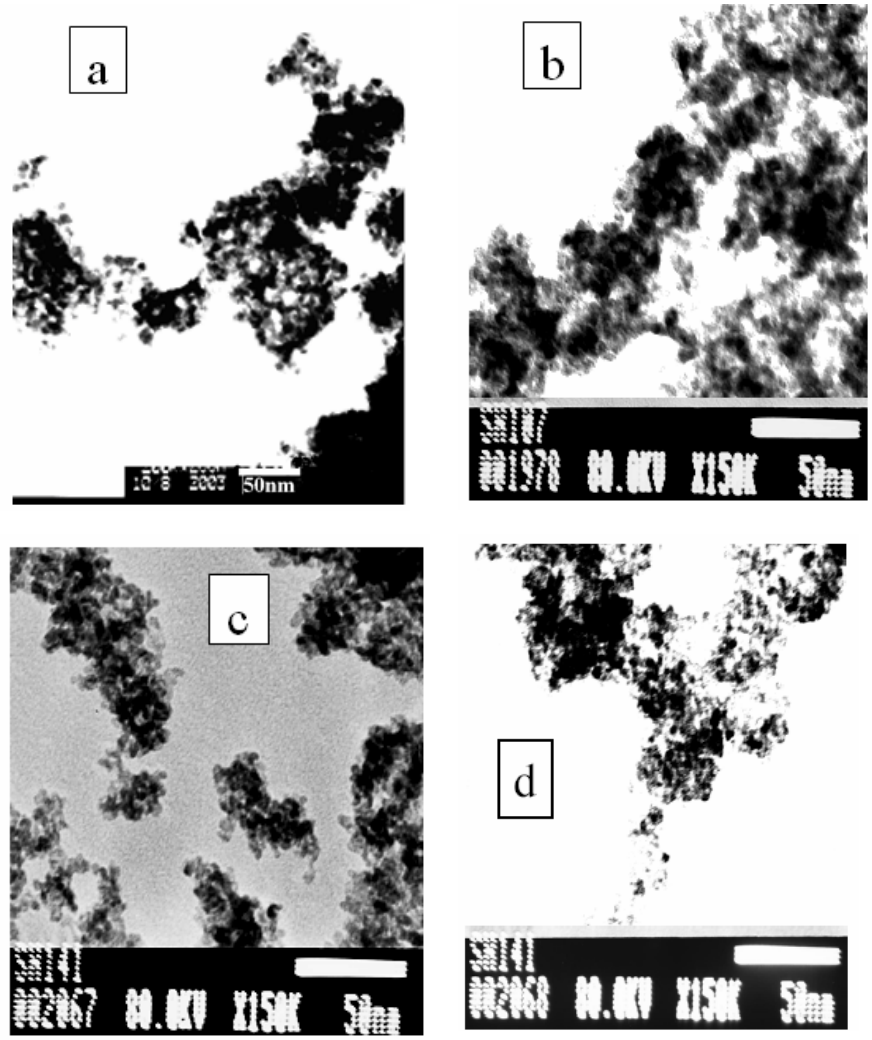

Figure 7. TEM micrographs of N(x)773/378-CeO_2 samples (a) x = 1.0, (b) x = 2.2, (c) x = 3.3, and (d) x = 5.5.

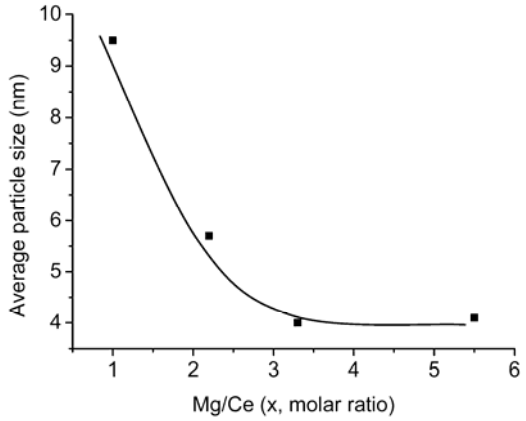

Figure 8. Effect of Mg/Ce(x) on the particle size of N(x)773/378-CeO_2 samples.

Figure 9 shows the effect of x on the surface area (S_g) of the leached and annealed samples of N(x)773/773-CeO_2 and N(x)1253/1253-CeO_2. The S_g increased with x increasing, and approached constant when $x \geq a$ given value of x_0. The x_0 was about 2.2 and 5.5, respectively, for $Tc = Ta = 773$K and 1253K. These results are consistent with the crystallite size results and particle size results (Figure 8), indicating that the effect of MgO on the S_g is mainly caused by the effect on the particle size.

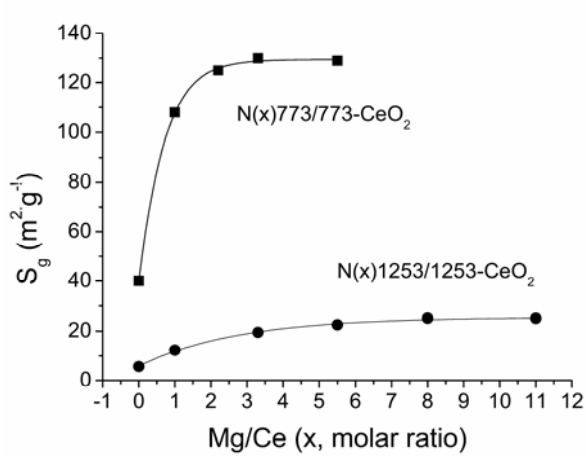

Figure 9. Effect of Mg/Ce(x) on the surface area (S_g) of ceria sample (a) N(x)773/773-CeO_2, and (b) N(x)1253/1253-CeO_2.

Based on the ceria crystallite size data from XRD results for N(x)773/773-CeO_2 (x = 0-5.5), a theoretic specific surface area (S_{cal}) was calculated through the following equation [19]:

$$S_{cal} = 6/D\rho = 824.17/D\ (m^2/g). \quad (1)$$

Wherein, D is crystallite size (nm) from XRD results; and ρ is the theoretical density of CeO_2 (7.28g/cm^3). S_{cal} represents the surface area of a single ceria crystallite. In some extent, S_g/S_{cal} reflects the dispersity of the ceria samples. As shown in Figure 10, S_g/S_{cal} increased with x increasing, and approached constant when $x \geq 3.3$, consistent with the trends in Figures 8 and 9. These results indicate that, the existence of MgO hampers the ceria particles and/or crystallites from agglomerating.

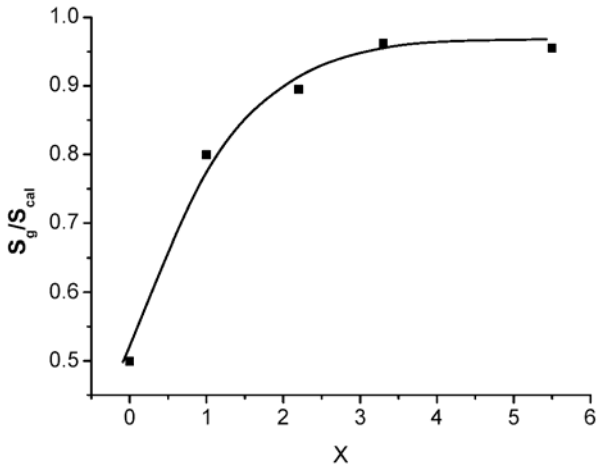

Figure 10. Effect of Mg/Ce(x) on the dispersity of N(x)773/773-CeO_2 samples.

The effect of MgO on the S_g of ceria might be explained as follows. In the gel calcining process, the formed ceria particles might be isolated by the formed MgO particles. With Mg/Ce increasing, more and more MgO particles acted as isolators between the CeO_2 particles, so that CeO_2 particles could not contact each other and agglomerated to form large particles. Therefore, the S_g of resulting ceria increased with Mg/Ce increasing. When Mg/Ce increased to the given value of x_0, the ceria

particles might be surrounded completely by MgO particles, so that, further increase of Mg/Ce had no apparent effect on the S_g of ceria. Since, the size of the formed MgO particles and thus, the space between the MgO particles would increase with increasing the calcining temperature, the resulting ceria particles in the space between MgO particles would also increase in size with increasing calcining temperature. Since, the annealing process took place at a temperature equal to or lower than the calcining temperature, the trend of the effect of Mg/Ce and the calcining temperature on the S_g of ceria was not changed by the annealing process.

In the gel calcining process, the newly formed nano-ceria particles were isolated by MgO particles; therefore, they could not agglomerate into larger particles, but could be thermally stabilized in the rest calcining process. Consequently, the obtained nano-ceria power showed higher thermal stability than the ceria prepared with the conventional methods [20, 21, 22].

4. Conclusions

A new method and its mechanism for the preparation of nano-ceria powder of high thermal stability were studied. The calcining process mainly included two weight-loss steps. The lower temperature step might be due to the reaction between the organic fragments and nitrogen oxides, and the catalytic function of MgO. The higher temperature step was due to the reaction between the organic fragments and O_2, and the catalytic function of CeO_2. The MgO in the mixed powder could be completely removed by reaction with acetic acid solution (2.5%), but the CeO_2 remained unaffected. In the calcining process, the freshly formed ceria particles could thermally be stabilized in the rest calcining, but did not agglomerate because the formed MgO particles might act as isolators. Consequently, the resulting ceria showed high surface area and high thermal stability.

References

[1] E. Aneggi, C. Leitenburg, G. Dolcetti and A. Trovarelli, Catalysis Today 136 (2008), 3.

[2] P. L. Chen and I.-W. Chen, J. Am. Ceram. Soc. 76 (1993), 1577.

[3] M. L. Dos Santos, R. C. Lima, C. S. Riccardi, R. L. Tranquilin, P. R. Bueno, J. A. Varela and E. Longo, Materials Letters 62 (2008), 4509.

[4] T. H. Etsell and S. N. Flengas, Chem. Rev. 70 (1970), 339.

[5] H. N. Evin, G. Jacobs, J. Ruiz-Martinez, U. M. Graham, A. Dozier, G. Thomas and B. H. Davis, Catalysis Letters 122(1-2) (2008), 9-19.

[6] T. Garcia, B. Solsona and S. H. Taylor, Catalysis Letters 105 (2005), 183.

[7] P. Janos and M. Petrak, J. Mater. Sci. 26 (1991), 4062.

[8] T. Kudo and H. Obayashi, J. Electrochem. Soc. 123 (1976), 415.

[9] R. X. Li, S. Yabe, M. Yamashita, S. Momose, S. Yoshida, S. Yin and T. Sato, Solid State Ionics 151 (2002), 235.

[10] T. Masui, K. Fujiwara, K.-I. Machida and G.-Y. Adachi, Chem. Mater. 9 (1997), 2197.

[11] S. Matsumoto, Catalysis Today 90 (2004), 183.

[12] B. R. Powell, R. L. Bloink and C. C. Erckel, J. Am. Ceram. Soc. 71 (1988), 104.

[13] G. R. Rao, P. Fornasiero, R. Di Monte, J. Kaspar, G. Vlaic, G. B. Alducci, S. Meriani, G. Gubitosa, A. Creemona and M. Graziani, J. Catal. 162 (1996), 1.

[14] T. Tsuzuki and P. G. McCormick, J. Am. Ceram. Soc. 84 (2001), 1453.

[15] X. Wang and R. J. Gorte, Catalysis Letters 73 (2001), 15.

[16] F.-Y. Wang, G.-B. Jung, A. Su, S.-H. Chan, X.-A. Li, M. Duan and Y.-C. Chiang, Materials Letters 63 (2009), 952-954.

[17] L. X. Yin, Y. Q. Wang, G. S. Pang, Y. Koltypin and A. Gedanken, J. Colloid Interface Sci. 246 (2002), 78.

[18] M. Zawadzki, Journal of Alloys and Compounds 454 (2008), 347.

[19] Y.-W. Zhang, R. Si, C.-S. Liao, C.-H. Yan, C.-X. Xiao and Y. Kou, J. Phys. Chem. B 107 (2003), 10159.

[20] U. S. Patent No. 3, 830, 758.

[21] U. S. Patent No. 4, 661, 330.

[22] E. P. Patent No. 0, 444.470 A1

■